COMPDYN 2013
4th ECCOMAS Thematic Conference on
Computational Methods in Structural Dynamics and Earthquake Engineering
M. Papadrakakis, V. Papadopoulos, V. Plevris (eds.)
Kos Island, Greece, 12–14 June 2013

THE APPLICATION OF FEM/DEM METHOD IN ANALYSIS OF RC BEAM-COLUMN JOINTS

Željana Nikolić[1*], Nikolina Živaljić[1] and Hrvoje Smoljanović[1]

[1] Faculty of Civil Engineering, Architecture and Geodesy, University of Split
Matice hrvatske 15, 21000 Split
e-mail: zeljana.nikolic@gradst.hr; nikolina.zivaljic@gradst.hr; hrvoje.smoljanovic@gradst.hr

Keywords: Combined finite-discrete element method (FEM/DEM), Reinforced beam-column joint, Monotonic loading, Cyclic loading.

Abstract. *One of very interesting problem in civil engineering applications is reinforced concrete beam-column joints subjected to monotonic and cyclic load. Predicting of the behaviour of reinforced concrete beam-column joints under monotonic and cyclic loading imposes the need to develop numerical model which will be able to include effects of the behaviour of reinforced concrete structures due to dynamic action in linear elastic stage, crack initiation and propagation, energy dissipation mechanisms due to non linear effects, inertial effects due to motion, contact impact and finally to attain state of the rest that is a consequence of energy dissipation mechanisms in the system. It is possible to include all previously mentioned effects with the finite-discrete element method (FEM/DEM). In this paper, a robust numerical model of concrete reinforcement, which is based on approximation of the experimental curves for behaviour of the concrete and steel in crack, is aimed to predict the behaviour of reinforced concrete beam-column joints subjected to monotonic and cyclic load. Cracking of the structure is enabled by discrete model of cracks where the cyclic behaviour of concrete and steel was implemented. The development of the cracks is analyzed for mid and end RC beam-column joints.*

1 INTRODUCTION

For predicting the behaviour and collapse of reinforced concrete structures, the numerical model should be able to include effects of the behaviour of concrete structures due to dynamic action in linear elastic stage, crack initiation and propagation, energy dissipation mechanisms due to non linear effects, inertial effects due to motion, contact impact and finally to attain state of the rest that is a consequence of energy dissipation mechanisms in the system. It is possible to include all previously mentioned effects with the finite-discrete element method [1, 2].

There has been a number of fracture models proposed in the context of both discrete element methods and combined finite discrete element method. Some of the models are based on a global approach applied to each individual body, while others used a local smeared crack approach or local single-crack approach. In this work a model for plane crack initiation and crack propagation in concrete is used [3]. The model combines standard finite element formulation for the hardening part of the constitutive law with the single-crack model for the softening part of stress-strain curve. Finite elements are used to model behaviour of the material up to the ultimate tensile strength while a discrete crack model is used for modelling of the crack opening and separation along edges of finite elements.

In the model presented in this paper an embedded model of reinforcing bars [4, 5] is implemented in Y2D combined finite-discrete element code [6]. Cracking of the concrete is enabled by a combined single and smeared crack model. The concrete and reinforcing bars are analyzed separately, but they are connected by the relation between the size of the concrete crack and strain of the reinforcing bar [7]. Cyclic behaviour of the steel during the cyclic load is modelled with improved Kato's model [8].

In this paper the application of combined finite-discrete element method (FEM/DEM) in numerical analysis of reinforced beam-column joints is shown.

2 MODELLING OF THE REINFORCED CONCRETE STRUCTURE

In this work an embedded model of reinforcing bars is implemented in a combined finite-discrete element model based on Y2D-code. The concrete structure is discretized on triangular finite elements, while the reinforcing bars are modelled with linear one-dimensional elements which can be placed in arbitrary position inside the concrete finite elements. The model of the reinforced concrete structure with the embedded reinforcing bar is shown in Figure 1.

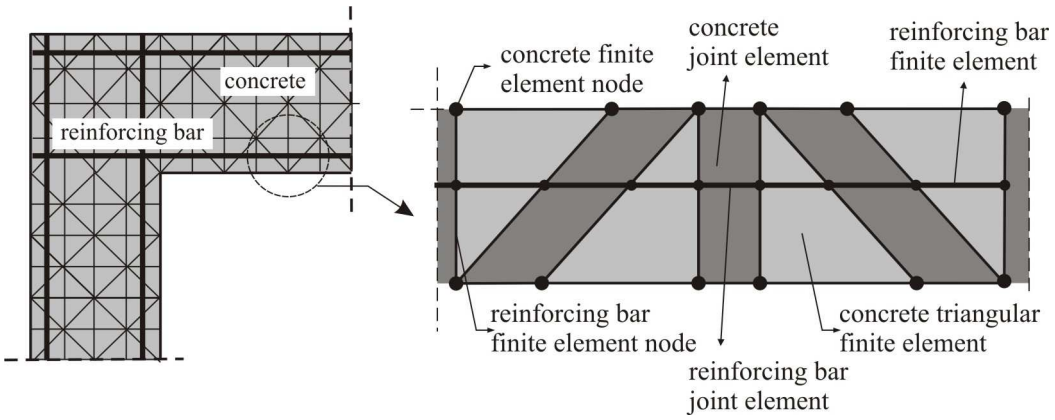

Figure 1: Discretization of reinforced concrete structure.

In the first step the reinforcement is modelled as bar (Figure 1). Intersection between the sides of concrete finite elements and reinforcing bars gives the reinforcement finite elements.

The structure behaves as continuum until opening of the crack. The deformation of the triangular element influence to the deformation of the reinforcing bars. When the crack in concrete appears, joint element in concrete as well as joint element in reinforcing bars is occurred. The concrete and reinforcing bars are analysed separately, but they are connected by the relationship between the size of the concrete crack and strain of the reinforcing bar.

2.1 Concrete model in joint element

In this work the concrete model is based on crack initiation and crack propagation of mode I and mode II loaded cracks [3]. The model is developed on the basis of experimental stress-strain curves for concrete in tension. The area under the stress-strain curve consists of two parts, first is the part used for modelling of the concrete behaviour up to the crack opening [3] while the second part represents strain softening after the tensile strength is exceeded [9]. The assumption of the discrete crack model is that the cracks coincide with the finite element edges. The total number of the nodes for each of the finite element meshes is doubled and the continuity between elements is realized through the penalty method [1]. Separation of the edges induces a bonding stress which is a function of the size separation δ [3].

No separation of the adjacent elements occurs before the tensile strength is reached, i.e. the edges of two adjacent elements are held together by normal and shear springs. Procedure of the separation of the elements and complete relationship for the normal and shear bonding stress are given in [3].

2.2 Steel material model in reinforcement joint element

In this work a model of the relationship between the concrete crack size and strain of the reinforcing bar developed by Shima [10] and Shin [7] is applied. The model is based on experimental strain-slip curves and represents well approximation of the behaviour of reinforcing bar with the expressed plastic strain caused by cyclic loading.

The steel strain-slip relation before the yielding of reinforcing bar is given by expressions:

$$s = \varepsilon_s (6 + 3500\varepsilon_s) \tag{1}$$

$$s = \left(\frac{S}{D}\right) \cdot K_{fc}, \quad K_{fc} = \left(\frac{f_c'}{20}\right)^{2/3} \tag{2}$$

where $s = s(\varepsilon_s)$ is normalized steel slip, D is bar diameter and f_c' is concrete strength.

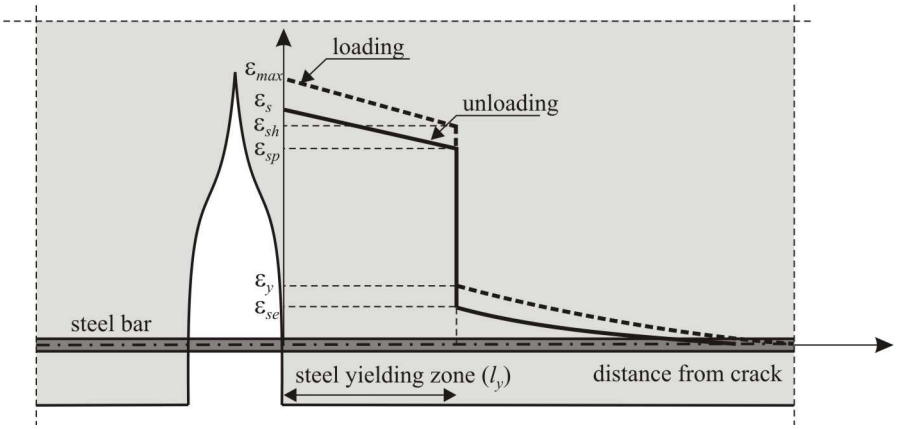

Figure 2: Strain distribution along the reinforcing bar in the post-yield range.

Normalized slip in the post-yield range is given by expression:

$$s = s_{pl} + s_e \tag{3}$$

where s_e is slip in the elastic region and s_{pl} is slip in the yield region. A strain distribution along the reinforcing bar in the post-yield region is shown in Figure 2, where ε_{se} is a strain at the yield boundary point on the elastic region and ε_{sp} is a strain at the yield boundary point on the yield region.

If the deformation of concrete is ignored, the steel slip can be determined by integration of the steel strain along the reinforcement axis. Normalized plastic steel slip in the yield region is given by an expression:

$$s_{pl} = \frac{(1+\beta)\varepsilon_s + \varepsilon_{sh} - \beta\varepsilon_{\max}}{\varepsilon_{\max} + \varepsilon_{sh}}(s_{\max} - s_y^*) \tag{4}$$

where $\beta = \sigma_{\max}/\sigma_y$ represents the gradient of the line shown in Figure 2, $\sigma_{\max}$ is the maximum stress in reinforcing bar under tensile loads, $s_{\max}$ is a function of $\varepsilon_{\max}$ and $s_y^* = \varepsilon_s(2+3500\varepsilon_s)$.

In the implemented model [11], calculation of shear force carried by the bar (Figure 3) is based on experimental curves [6] which describe curvature of the reinforcing bar in the vicinity of crack faces as function of deflection of the reinforcing bar at the interface t_s.

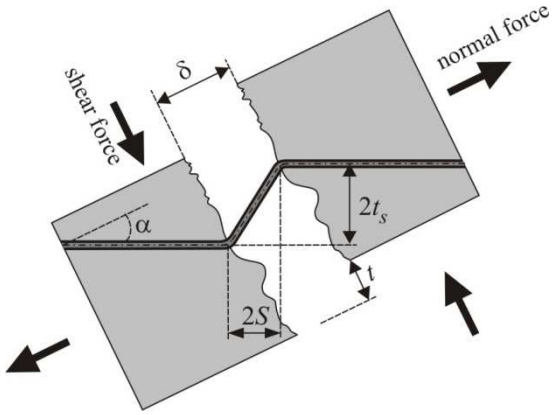

Figure 3: Discrete crack.

The effect of yield stress reduction due to the shear stress in the bar is taken into account by applying the Von Mises yield criterion and isotropic hardening rule as:

$$\sigma_y' = \sigma_y\sqrt{1-3\left(\tau_s/\sigma_y\right)^2} \tag{5}$$

where σ_y' is the reduced yield stress, τ_s is the shear stress of the reinforcing bar between the crack surfaces [11], which is obtained as:

$$\tau_s = \frac{V_s}{A_s} \tag{6}$$

where A_s is the cross-sectional area of the reinforcing bar.

The influence of adjacent cracks is approximately taken into account through a reduction factor α, which depends on crack distance l_{cr}. The steel slip s_{cr}, which considers the influence of adjacent cracks, is expressed for monotonic loading as:

$$s_{cr} = \alpha s \tag{7}$$

where s is non-dimensional slip defined by expression (14), while reduction factor α is given:

$$\alpha = 1 - e^{-(0.065 l_{cr}/D + 0.5)^3}, \quad \alpha \le 0.087 l_{cr}/D \tag{8}$$

In this work non-linear material model for steel is based on experimental stress-strain curve where cyclic behaviour of the steel during the cyclic load is modelled with improved Kato's model [6, 8].

3 EXAMPLES

The application of presented model for analysis of reinforced-concrete structures based on FEM/DEM method was performed in the numerical analysis of exterior and interior reinforced concrete beam-column joints.

3.1 Exterior RC beam-column joint

The application of presented numerical model is performed in the analysis of exterior RC beam-column joint subjected to monotonically increasing and cyclic load. The geometry characteristics of the RC beam-column joint are shown in Figure 4. Material characteristics are shown in Table 1.

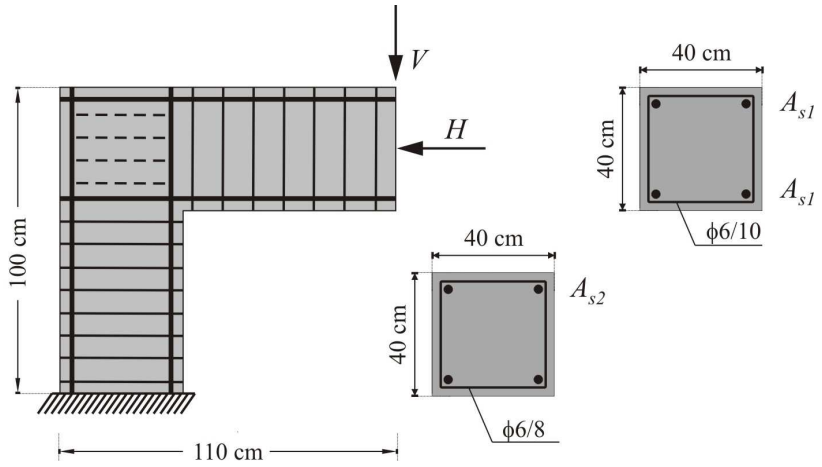

Figure 4: Geometry of exterior RC beam-column joint.

Concrete		Steel	
E_c (MPa)	29730	E_s (MPa)	210 000
ν	0.2	f_y (MPa)	400
f_t (MPa)	3.15	f_u (MPa)	500
f_c (MPa)	30.0	A_{s1} (m^2)	0.00026
G_f (N/m)	100	A_{s2} (m^2)	0.000452

Table 1: Material characteristics.

Exterior RC beam-column joint is reinforced in two different ways and subjected to monotonically increasing vertical and horizontal load with equal value. Initiation and propagation of the cracks in the RC beam-column and the ratio of vertical displacement at the collapse point v_c and vertical displacements at the moment when initial crack appears v_i for different reinforcement type were analyzed.

Failure patterns for two type of reinforcing are shown in figures 5 and 6.

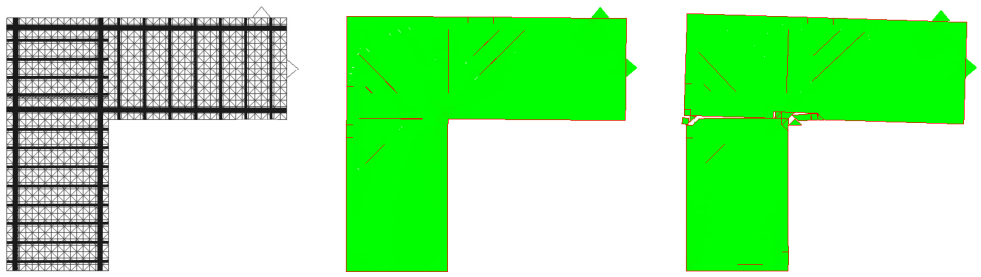

Figure 5: Beam-column joint reinforced with horizontal stirrups (reinforcing type I): (a) discretization, failure patterns for: (b) V=H=254.8 kN, (c) after V=H=268.2 kN.

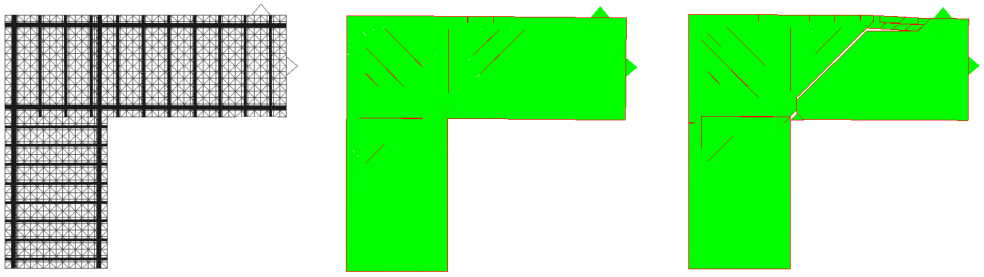

Figure 6: Beam-column joint reinforced with vertical stirrups (reinforcing type II): (a) discretization; failure patterns for: (b) V=H=265.3 kN, (c) after V=H=272.2 kN.

Figure 7 shows vertical load-displacement relation for two different types of reinforcing.

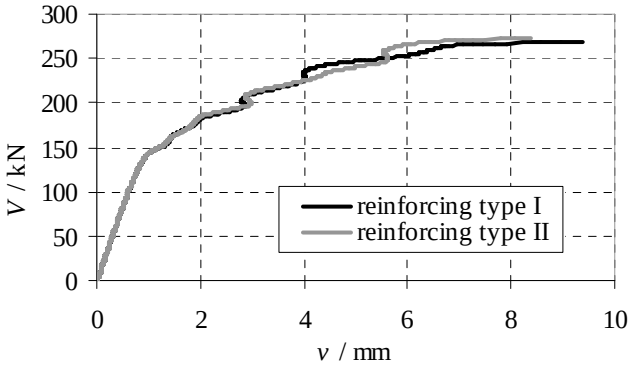

Figure 7: Vertical load - displacement relation.

The ratio of vertical displacement v_c at the collapse point and vertical displacements v_i at the moment when initial crack appears for different reinforcement type is shown in Table 2.

Reinforcing type	v_c / v_i
I	18.80
II	16.74

Table 2: Ratio v_c / v_i for each reinforcing type.

It can be seen that the larger vertical displacement was achieved for reinforcing type II. The greater capacity was achieved for reinforcing type II where the fracture is realized in the beam. Load capacity for beam-column joint reinforced with horizontal stirrups is 1.5% lower and dominant cracks occur at the top of the column.

Exterior RC beam-column joint, shown in Figure 4, is reinforced in two different ways and subjected to cyclic vertical and horizontal load (Figure 8). Initiation and propagation of the cracks in the RC beam-column and the ratio of vertical displacement at the moment of collapse v_c and vertical displacements v_i at the moment when initial crack appears for different reinforcement type were analyzed.

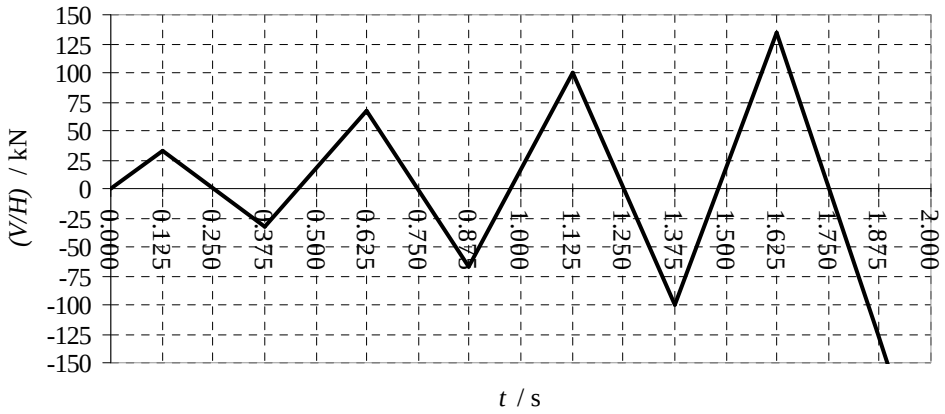

Figure 8: Load history.

Failure patterns for two type of reinforcing are shown in figures 9 and 10.

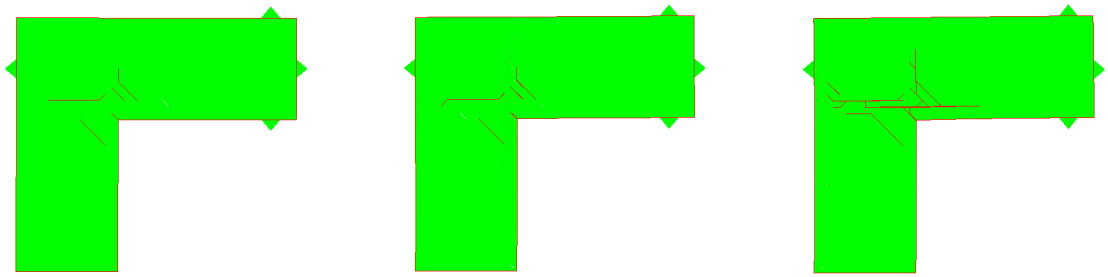

(a) (b) (c)

Figure 9: Failure patterns for exterior beam-column joint reinforced with horizontal stirrups: (a) t=1.375s, (b) t=1.850s, (c) t=1.860s.

For exterior beam-column joint reinforced with horizontal stirrups, first crack occurs in the third cycle of loading for the force of 75.7 kN. At the time of the collapse vertical force was 116.5 kN with maximum vertical displacement v=10.77 mm.

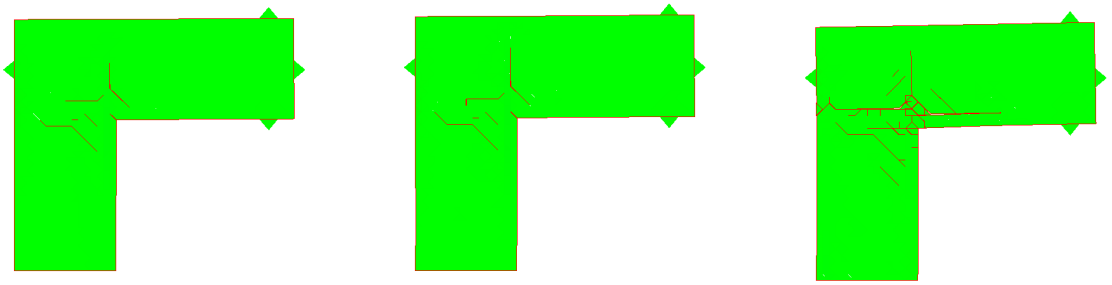

(a) (b) (c)

Figure 10: Failure patterns for exterior beam-column joint reinforced with vertical stirrups: (a) t=1.375s, (b) t=1.850s, (c) t=1.870s.

For exterior beam-column joint reinforced with vertical stirrups, first crack also occurs in the third cycle of loading for the force of 75.7 kN. At the collapse point vertical force was 127.3 kN with maximum vertical displacement v =15.55 mm.

Figure 11 shows cyclic vertical load-displacement relation for two different types of reinforcing.

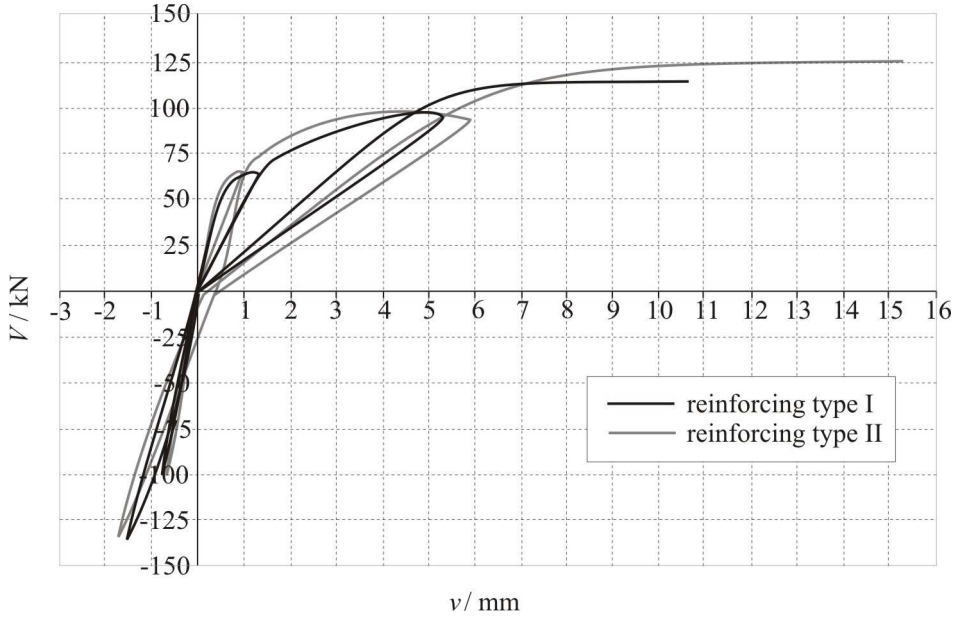

Figure 11: Vertical load - displacement relation.

The ratio of vertical displacement at the moment of collapse v_c and vertical displacement v_i at the moment when initial crack appears for different reinforcement type is shown in Table 3.

Reinforcing type	v_c / v_i
I	21.53
II	31.01

Table 3: Ratio of v_c / v_i for each reinforcing type.

It can be seen that larger vertical displacement and greater capacity was achieved for reinforcing type II. For the beam-column joint reinforced with horizontal stirrups (reinforcing type I) load capacity is 8.5% lower in regards to reinforcing type II.

3.2 Interior RC beam-column joint

The application of presented numerical model is performed in the analysis of interior RC beam-column joint subjected to monotonically increasing and cyclic load. The geometry characteristics of interior RC beam-column joint are shown in Figure 12. Material characteristics are shown in table 4.

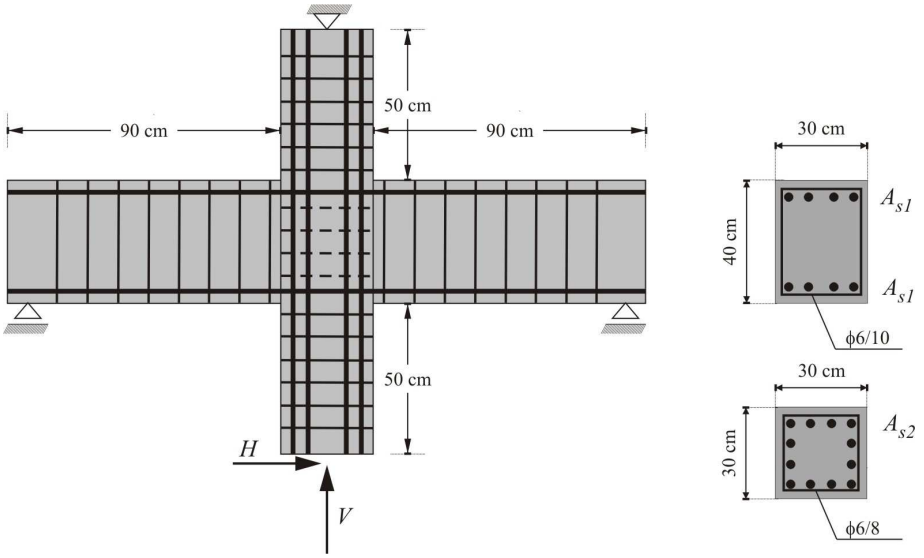

Figure 12: Geometry of interior RC beam-column joint.

Concrete		Steel	
E_c (MPa)	29730	E_s (MPa)	210 000
ν	0.2	f_y (MPa)	400
f_t (MPa)	3.15	f_u (MPa)	500
f_c (MPa)	30.0	A_{s1} (m^2)	0.000452
G_f (N/m)	100	A_{s2} (m^2)	0.001357

Table 4: Material characteristics.

Interior RC beam-column joint is reinforced in three different ways and subjected to monotonically increasing horizontal load and constant vertical force V=700 kN. Initiation and propagation of the cracks in the interior RC beam-column and the ratio of horizontal displacement at the moment of collapse u_{Hc} and horizontal displacements at the moment when initial crack u_{Hi} appears for different reinforcement type were analyzed.

Failure patterns at the collapse point for three different types of reinforcing are shown in figures 13, 14 and 15.

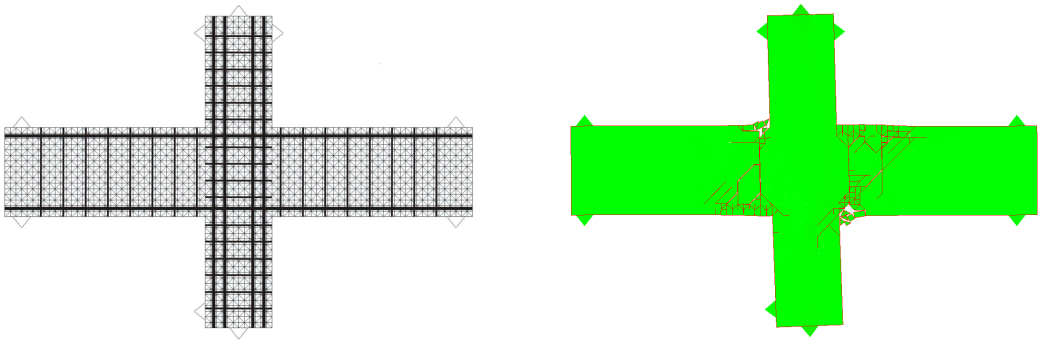

(a) (b)

Figure 13: Interior beam-column joint reinforced with horizontal stirrups: (a) discretization, (b) failure patterns for H=216.8 kN.

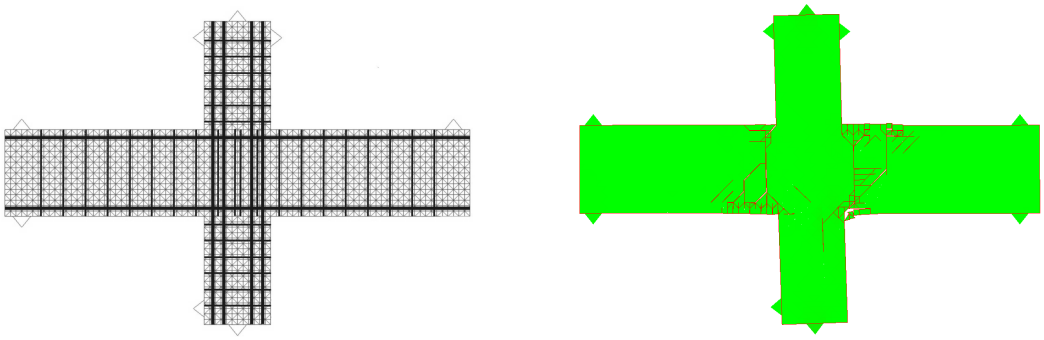

(a) (b)

Figure 14: Interior beam-column joint reinforced with vertical stirrups: (a) discretization, (b) failure patterns for H=215.13 kN.

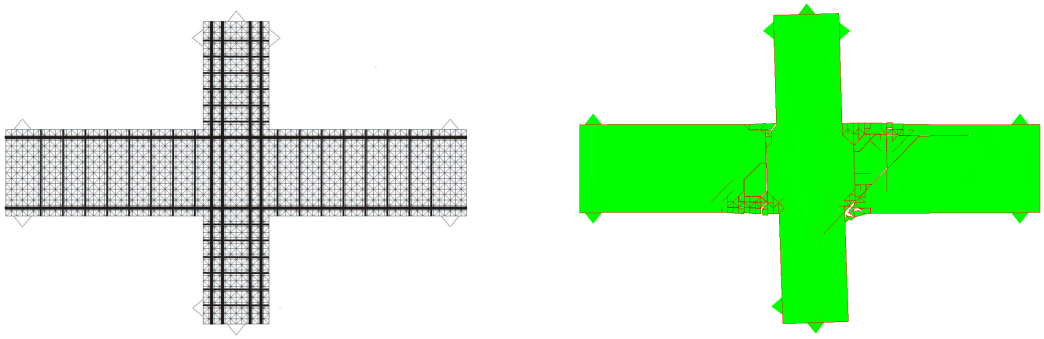

(a) (h)

Figure 15: Interior beam-column joint without stirrups: (a) discretization, (b) failure patterns for H=216.4 kN.

Figure 16 shows horizontal load-displacement relation for three different types of reinforcing.

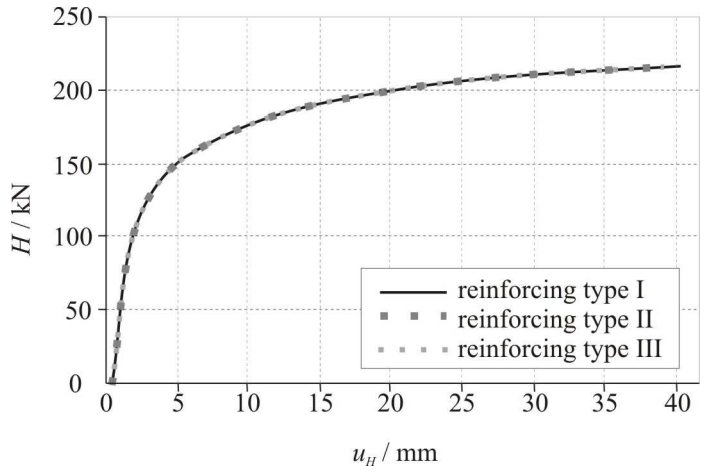

Figure 16: Horizontal load – displacement relation

The ratio of horizontal displacement at the moment of collapse u_{hc} and horizontal displacement at the moment when initial crack appears u_{Hi} for different reinforcement type are shown in Table 5.

Reinforcing type	u_{Hc} / u_{Hi}
I	42.10
II	39.94
III	41.10

Table 5: Ratio u_{Hc} / u_{Hi} for each reinforcing type.

It can be seen that the capacity for all three types of reinforcement is equal. The highest difference in capacity between these cases is 1.0% and the cracks propagated through the beam which is convenient to the structure.

Interior RC beam-column joint, shown in Figure 12, is reinforced in three different ways (Figures 13,14,15) and subjected to constant vertical force V=700 kN and cyclic horizontal load (Figure 17).

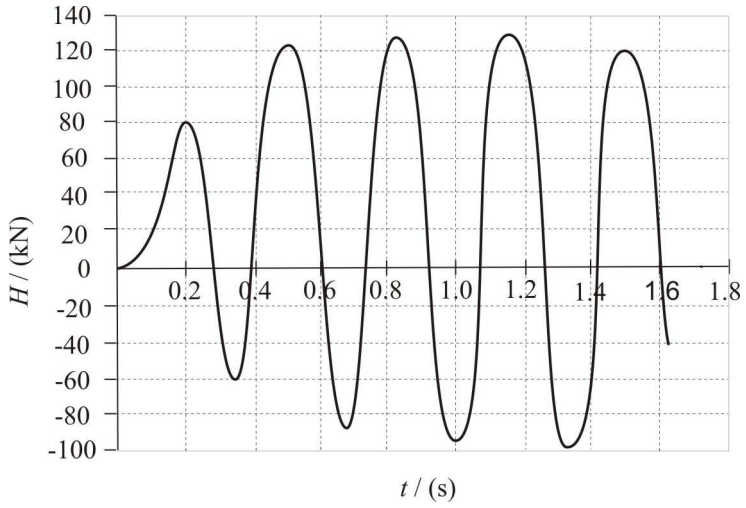

Figure 17: History load for interior beam-column joint.

Initiation and propagation of the cracks in the interior RC beam-column and the ratio of the horizontal displacement at the collapse point u_{hc} and horizontal displacements at the moment when the initial crack appears u_{Hi} for different reinforcement types were analyzed.

Failure patterns for three type of reinforcing are shown in figures 18, 19 and 20.

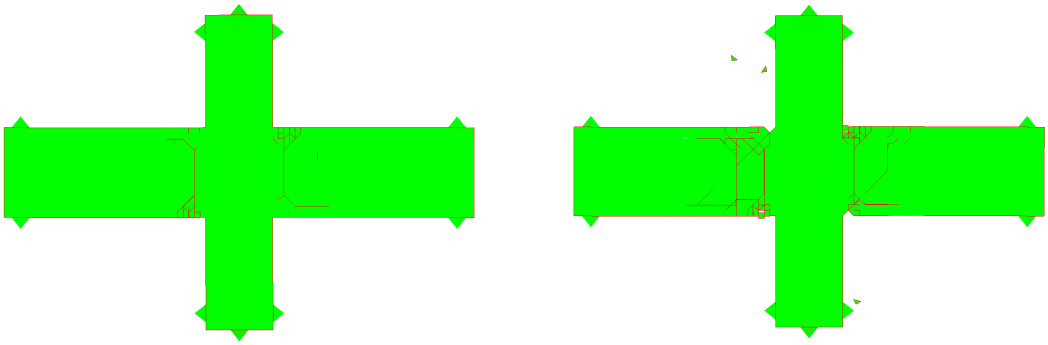

(a) (b)

Figure 18: Failure patterns for interior beam-column joint reinforced with horizontal stirrups: (a) t=1.083s, (b) t=1.61s.

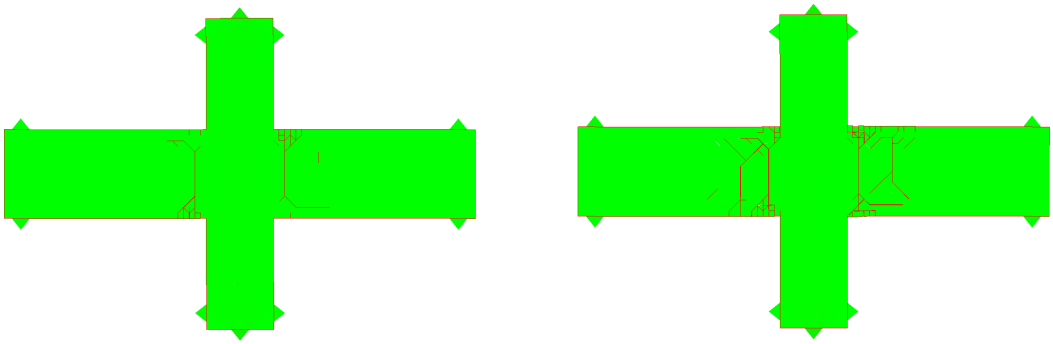

(a) (b)

Figure 19: Failure patterns for interior beam-column joint reinforced with vertical stirrups: (a) t=1.083s, (b) t=1.61s.

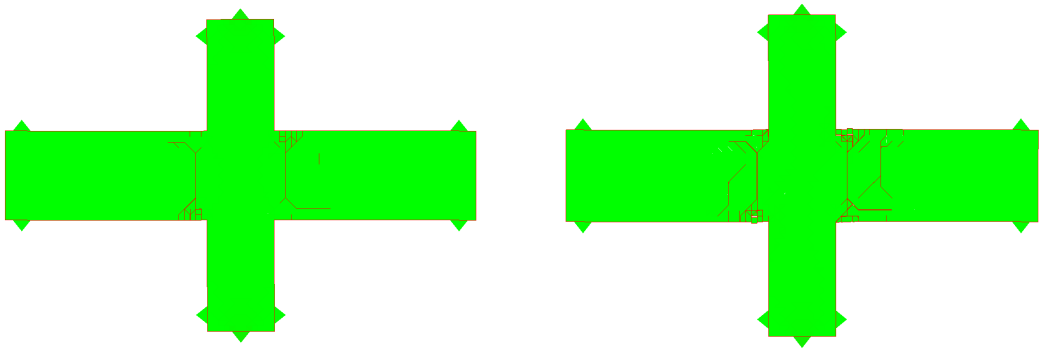

(a) (b)

Figure 20: Failure patterns for interior beam-column joint without stirrups: (a) t =1.083s, (b) t =1.61s.

Figure 21 shows cyclic horizontal load-displacement relation for three different types of reinforcing. Very similar behaviour is achieved for all three types of reinforcing, as it is shown in figure 21.

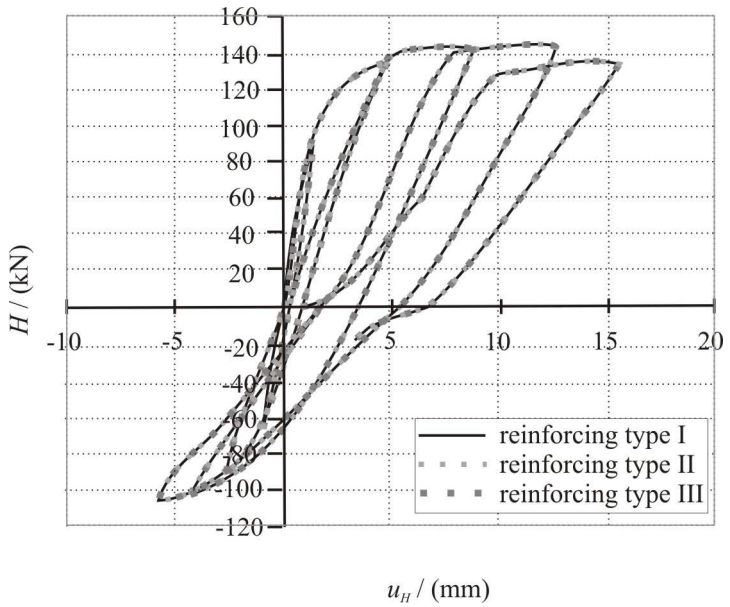

Figure 21: Horizontal load - displacement relation.

The ratio of the horizontal displacement u_{Hc} at the collapse point and horizontal displacement u_{Hi} at the moment when initial crack appears for different reinforcement type is shown in Table 6.

Reinforcing type	u_{Hc} / u_{Hi}
I	17.37
II	17.39
III	17.40

Table 6: Ratio u_{Hc} / u_{Hi} for each reinforcing type.

It can be seen that the highest degree of damage is achieved for the reinforcing type I, although load-displacement relation for all three types of reinforcing shows very similar behaviour. So it can be concluded that the influence of reinforcement is dominant in all cases.

4 CONCLUSIONS

- This paper presents the application of numerical model for reinforced concrete structures based on combined finite discrete element method in monotonic and cyclic loading of reinforced beam-column joints.
- The developed numerical model is based on embedded model of reinforcing bars, an approximation of the experimental curves for behaviour of the concrete and steel in crack and the interaction between the reinforcement and concrete which was taken into consideration by steel strain-slip relation. Cracking of the structure is enabled by discrete model of cracks where the cyclic behaviour of concrete and steel was implemented.
- RC beam-column joint is reinforced in three different ways: with the horizontal and vertical stirrups and without the stirrups. The analysis of exterior beam-column joint shows

larger bearing capacity for the reinforcing with vertical stirrups in joint. In interior beam-column joint almost identical load-displacement curve for all three types of reinforcing are obtained. The highest degree of damage is achieved for reinforcing with horizontal stirrups.

5 REFERENCES

[1] A. Munjiza, *The combined finite-discrete element method*, John Wiley & Sons, 2004.

[2] A. Munjiza, D.R.J. Owen, N. Bicanic, A combined finite-discrete element method in transient dynamics of fracturing solids. *Engineering Computations*, 12, 145-174, 1995.

[3] A. Munjiza, K.R.F. Andrews and J.K. White, Combined single and smeared crack model in combined finite-discrete element method. *Int. J. for Numerical Methods in Engineering*, 44, 41-57, 1999.

[4] N. Živaljić; Ž. Nikolić, A.Munjiza, A Combined Finite Discrete Element Model for Reinforced Concrete under Seismic Load. E. Onate, R. Owen, Đ. Perić, B. Suarez eds. COMPLAS XI, Barcelona, 2011.

[5] Ž. Nikolić and A. Mihanović, Non-linear finite element analysis of post-tensioned concrete structures, *Engineering Computations*, 14, 509-528, 1997.

[6] N. Živaljić, H. Smoljanović, Ž. Nikolić, A combined finite-discrete element model for RC structures under dynamic loading. *Engineering computations 2013* (accepted for publication).

[7] H. Shin, K. Maekawa, H. Okamura, Analytical approach of RC members subjected to reversed cyclic in plane loading. *Proceeding of JCI Colloquium on Ductility of Concrete Structures and its Evaluation*, 245-256, 1988.

[8] B. Kato, Mechanical properties of steel under load cycles idealizing seismic action. *Bulletin D'Information, AICAP-CEB symposium*, Rome, 131, 7-27, 1979.

[9] D.A. Hordijk, Tensile and tensile fatigue behaviour of concrete – experiments, modelling and analyses. *Heron*, 37, 3-79, 1992.

[10] H. Shima, L. Chou and H. Okamura, Micro and macro model for bond behaviour in RC, *Journal of the Faculty of Engineering*, The University of Tokyo, 39, 133-94, 1987.

[11] N. Živaljić, Finite-discrete element method for 2D seismic analysis of reinforced concrete structures, PhD thesis, University of Split, Croatia, 2012.